

Nanoscale

Accepted Manuscript



This is an *Accepted Manuscript*, which has been through the Royal Society of Chemistry peer review process and has been accepted for publication.

Accepted Manuscripts are published online shortly after acceptance, before technical editing, formatting and proof reading. Using this free service, authors can make their results available to the community, in citable form, before we publish the edited article. We will replace this *Accepted Manuscript* with the edited and formatted *Advance Article* as soon as it is available.

You can find more information about *Accepted Manuscripts* in the [Information for Authors](#).

Please note that technical editing may introduce minor changes to the text and/or graphics, which may alter content. The journal's standard [Terms & Conditions](#) and the [Ethical guidelines](#) still apply. In no event shall the Royal Society of Chemistry be held responsible for any errors or omissions in this *Accepted Manuscript* or any consequences arising from the use of any information it contains.

Cite this: DOI: 10.1039/c0xx00000x

www.rsc.org/xxxxxx

ARTICLE TYPE

Cu_{2-x}Se@mSiO₂-PEG Core-Shell Nanoparticles: a Low-Toxic and Efficient Difunctional Nanoplatfom for Chemo-Photothermal Therapy under Near Infrared Light Radiation with a Safe Power Density

Xijian Liu,^{‡ab} Qian Wang,^{‡ac} Chun Li,^a Rujia Zou,^{ad} Bo Li,^a Guosheng Song,^a Kaibing Xu,^a Yun Zheng^e and Junqing Hu^{*a}

Received (in XXX, XXX) Xth XXXXXXXXX 20XX, Accepted Xth XXXXXXXXX 20XX

DOI: 10.1039/b000000x

A low-toxic difunctional nanoplatfom integrating both photothermal therapy and chemotherapy for killing cancer cells using Cu_{2-x}Se@mSiO₂-PEG core-shell nanoparticles is reported. Silica coating and further PEG modifying improve the hydrophilicity and biocompatibility of copper selenide nanoparticles. As-prepared Cu_{2-x}Se@mSiO₂-PEG nanoparticles not only display strong near infrared (NIR) region absorption and good photothermal effect, but also exhibit excellent biocompatibility. The mesoporous silica shell is provided as the carrier for loading anticancer drug, doxorubicin (DOX). Moreover, the release of DOX from Cu_{2-x}Se@mSiO₂-PEG core-shell nanoparticles can be triggered by pH and NIR light, resulting in a synergistic effect for killing cancer cell. Importantly, the combination of photothermal therapy and chemotherapy driven by NIR radiation with safe power density significantly improves the therapeutic efficacy, and demonstrates better therapeutic effects for cancer treatment than individual therapy.

Keywords: Cu_{2-x}Se@mSiO₂, low-toxic, chemotherapy, controllable release, photothermal

1. Introduction

Photothermal therapy (PTT) that uses optical absorbing agents to “cook” cancer cells under light irradiation without damaging surrounding healthy tissue has attracted significant attention in recent years as a promising alternative or supplement to traditional cancer therapies.¹⁻³ Ideal PTT agents should exhibit strong absorbance in the near-infrared (NIR) region ($\lambda = 700-1300$ nm), which is a therapeutic window due to high optical transparency of biological tissues,⁴ and could efficiently transfer the absorbed NIR optical energy into heat. Furthermore, the PTT agents should have good biocompatibility.^{1,2} Currently, a series of NIR-light-absorbing nanomaterials have shown potential in PTT cancer treatment, such as gold nanorods,^{5,6} gold shells,^{7,8} gold cages,⁹⁻¹² palladium nanosheets,^{13,14} carbon nanotubes,^{15,16} graphene,^{17,18} polypyrrole,^{1,2} indocyanine dye,¹⁹ W₁₈O₄₉ nanowires,²⁰ copper sulfide,²¹⁻²⁴ and copper selenide nanoparticles.²⁵ However, one of the major limitations of using PTT for clinical cancer treatment is the relatively high treatment power density of laser for the aim of obtaining sufficient heating in cancer cell killing, which probably hurts normal tissues.²⁶ For clinical applications, the energy input of laser should be safe to avoid damage to healthy tissues and skins, which is always a primary concern for PTT. If PTT agents can integrate photothermal therapy and other treatment modalities into a single

noplatfom for cancer destruction, the treatment power density of laser will be effectively reduced, and skins and normal tissues can be avoided from harm. Numerous good results showed that the combination of photothermal therapy and chemotherapy had better effects on destroying cancer cells than chemotherapy or photothermal therapy alone due to the synergistic effect. For instance, Au@SiO₂,^{27,28} Cu₉S₅@SiO₂,²⁹ hollow mesoporous silica@Pd (HMSS-NH₂@ Pd),³⁰ Pd@Ag@sSiO₂@mSiO₂-DihBen,³¹ graphene@mSiO₂ (GSPI)³², DOX/ICG@lipid-polymer (DINPs)³³ and Fe₃O₄@PPy³⁴ nanocomposites have been fabricated and showed remarkable cancer-cell killing efficiency. Therefore, the development of such novel multifunctional treatment systems combining photothermal therapy and chemotherapy with safe and efficient therapeutic effect is vital.

Recently, copper selenide has been supposed to be a promising candidate as a photothermal agent due to high photothermal conversion efficiency and simple synthesis method.^{24,35} However, copper selenide is hydrophobic and less biocompatible when synthesized via hot injection. Though the copper selenide was coated by polymer, a suspicious long-term toxicity in vitro²⁵ still limited its applications in vivo therapy. Therefore, new methods of surface modification should be developed to further reduce the toxicity of copper selenide as PTT agents. Mesoporous silica nanoparticles (MSNs), which have shown excellent stability, non-cytotoxicity, tunable porosity

and facile modification,^{30,36} appeal researchers to use them as a nanocarrier for multifunctional drug delivery in drug controllable release area. Thus mesoporous silica coating is a very efficient way to reduce toxicity of photothermal materials, and to be used as anticancer drug carriers. So the combination of chemotherapy and photothermal therapy in a platform will be achieved by mesoporous silica coating.

In this work, we designed and prepared $\text{Cu}_{2-x}\text{Se}@m\text{SiO}_2\text{-PEG}$ core-shell nanoparticles by combining hot injection reaction and sol-gel reaction, and then by surface modification with PEGylation. Because the Cu_{2-x}Se nanoparticles core can effectively convert NIR light into fatal heat due to the strong surface plasmon resonance (SPR) absorption, and the biocompatible mesoporous silica shell can provide the carrier for loading anticancer drug, as-prepared $\text{Cu}_{2-x}\text{Se}@m\text{SiO}_2\text{-PEG}$ core-shell nanoparticles can be used as a low-toxic difunctional nanoplatform integrating both photothermal therapy and chemotherapy for killing cancer cells under NIR radiation. In particular, the low pH in cellular endosomes and the heat generated by the NIR irradiation can lead to rapid release of the DOX molecules loaded inside the mesoporous SiO_2 shells and enhance the chemotherapeutic effects of DOX. $\text{Cu}_{2-x}\text{Se}@m\text{SiO}_2\text{-PEG}$ core-shell nanoparticles as a difunctional nanoplatform for chemo-photothermal therapy have at least three important features: (1) Unlike chemo-photothermal therapy nanoplatforms based on noble-metal nanostructures that are limited by the high cost of noble-metal, $\text{Cu}_{2-x}\text{Se}@m\text{SiO}_2\text{-PEG}$ nanoplatform is benefited from its low cost and simple synthetic route. (2) $\text{Cu}_{2-x}\text{Se}@m\text{SiO}_2\text{-PEG}$ nanoplatform has an absorbance peak close to 980 nm, and guarantees high photothermal conversion ability when driven by the 980 nm laser. Also, the 980 nm light has deeper penetration depth in biological tissues than 808 nm light, and $\text{Cu}_{2-x}\text{Se}@m\text{SiO}_2\text{-PEG}$ nanoplatform has good PTT effect when is driven at safe power density of 0.72 W/cm^2 (higher than the 808 nm laser limit intensity set). (3) The $\text{Cu}_{2-x}\text{Se}@m\text{SiO}_2$ composites are modified by PEG, improving their colloidal stability and biocompatibility and decreasing immunogenicity in vivo therapy. In our vitro and vivo experiments, the combination of photothermal therapy and chemotherapy significantly improves the therapeutic efficacy, and displays better therapeutic effects for cancer treatment than individual therapy.

2. Experimental Section

2.1. Chemicals and reagents. All reagents were used without further purification. Copper (I) chloride (CuCl), cetyltrimethylammonium bromide (CTAB), sodium hydroxide (NaOH) and anhydrous ethanol are analytically pure and were purchased from Sinopharm Chemical Reagent Co. (Shanghai, China), and tetraethylorthosilicate (TEOS, GR), selenium powders, oleic acid, oleylamine (approximate C18 from 80-90%) were obtained from Aladdin, and 2-[Methoxy(polyethyleneoxy)propyl]-trimethoxysilane (PEG-silane, MW = 596-725 g/mol, 9-12 EO) was obtained from Gelest (Morrisville, PA) and doxorubicin hydrochloride (DOX) was got from Huafeng United Technology CO., Ltd. (Beijing, China)

2.2. Characterization. Sizes, morphologies, and microstructures of the nanoparticles were determined by a transmission electron

microscope (TEM; JEM-2100F). Powder X-ray diffraction (XRD) was conducted by a D/max-2550 PCX-ray diffractometer (Rigaku, Japan). The surface area, pore size, and pore-size distribution of the products were determined by Brunauer-Emmett-Teller (BET) nitrogen adsorption-desorption and Barrett-Joyner-Halenda (BJH) methods (Micromeritics, ASAP2020). Fourier transform infrared (FTIR) spectra were measured using an IRPRESTIGE-21 spectrometer (Shimadzu) using the KBr pressed pellets. UV-visible absorption spectra were measured on UV-Vis 1901 Spectrophotometer (Phoenix) using quartz cuvettes with an optical path of 1 cm. Content of copper ions and Au ions in the solution was determined by a Leeman Laboratories Prodigy high-dispersion inductively coupled plasma atomic emission spectroscopy (ICP-AES).

2.3. Synthesis of Cu_{2-x}Se nanocrystal. Cu_{2-x}Se nanocrystals were prepared by a modified thermal injection method described previously.³⁵ In a typical procedure, 39.5 mg of selenium powders and 5 mL of oleic acid (OA) in a flask were heated at 120°C with flowing nitrogen for 30 min in order to remove any moisture and oxygen and subsequently were heated to 280°C under magnetic stirring for 30 min. Then Se-OA precursor was synthesized for followed use. In another flask, the mixtures of 5 mL of OA, 5 mL of oleylamine (OAM) and 49.5 mg of CuCl were heated at 120°C with flowing nitrogen for 30 min and subsequently were heated to 220°C under magnetic stirring. Then 5 mL of Se-OA precursor was injected into the above copper precursors, forming dark solution immediately, and then was maintained at 220°C for 5 min. Subsequently the reaction solution rapidly cooled to 60°C . Then ethanol was added to the reaction solution followed by centrifuging at 12000 rpm for 10min. This procedure was repeated twice to remove residual surfactants. Finally, the Cu_{2-x}Se nanocrystals were dispersed in 10 mL of chloroform for later use.

2.4. Synthesis of CTAB-stabilized Cu_{2-x}Se nanocrystals ($\text{Cu}_{2-x}\text{Se-CTAB}$). A phase transfer of as-prepared Cu_{2-x}Se nanocrystals from chloroform to water proceeded by a modified method described previously.^{29, 39} First, the above 10 mL of chloroform solution containing the as-prepared Cu_{2-x}Se nanocrystals was mixed with CTAB solution (1.5 g CTAB in 75 mL of water). By vigorous stirring at 40°C for 36 h, a brown oil-in-water microemulsion formed, and then the chloroform was completely boiled off by rotary evaporation. Above solution was filtered through a $0.22 \mu\text{m}$ of millipore filter to remove impurities and then diluted to 75 mL with deionized water, forming in a transparent dark green solution of $\text{Cu}_{2-x}\text{Se-CTAB}$. In order to prevent CTAB precipitation, the filtration of process and store of $\text{Cu}_{2-x}\text{Se-CTAB}$ solution should be kept above 25°C .

2.5. Synthesis of $\text{Cu}_{2-x}\text{Se}@m\text{SiO}_2\text{-PEG}$ core-shell nanoparticles. The above 50 mL of the $\text{Cu}_{2-x}\text{Se-CTAB}$ solution was treated by ultrasonication and further continuously stirred for 1 h at 40°C . Then, 3 mL of ethanol and 100 μL of NaOH solution (30 mg/mL) were added to the above solution. After stirred for several minutes, 100 μL of TEOS was dropped into this mixture. The mixture was allowed to react for 1.5 h at 40°C under continuously stirring. Subsequently, 100 μL of PEG-silane was added under stirring for another 6.5 h and $\text{Cu}_{2-x}\text{Se}@m\text{SiO}_2\text{-PEG}$ core-shell nanoparticles mixture was obtained. The

synthesized product was centrifuged (12000 rpm, 10 min), washed with ethanol three times. Then the products were transferred to the ethanol solution of NH_4NO_3 (50 mL, 10 mg/mL) and stirred at 50 °C for 2 h, the template of CTAB was removed through ion exchange. After that, as-prepared $\text{Cu}_{2-x}\text{Se}@m\text{SiO}_2\text{-PEG}$ nanoparticles were washed with ethanol three times. The final products were dispersed into deionized water and stored at 4 °C for further use.

2.6. Measurement of photothermal performance.

Measurement of photothermal performance was referenced our previous method.²⁹ The $\text{Cu}_{2-x}\text{Se}@m\text{SiO}_2\text{-PEG}$ nanoparticles and Au nanorods aqueous dispersions (0.3 mL) of different concentrations (10, 25, 50, 100, 200, 400 mg/mL) were irradiated by laser (980 nm) for 8 min. The light source was an external adjustable power (0-0.3 W) 980 nm semiconductor laser device with a 5 mm diameter laser module (Xi'an Tours Radium Hirsh Laser Technology Co., Ltd. China). The output power density was independently calibrated using a handy optical power meter (Newport model 1918-C, CA, USA) and was found to be ~ 0.72 W/cm². The temperature of the solutions was measured by a digital thermometer (with an accuracy of 0.1 °C) with a thermocouple probe every 5 s.

2.7. DOX loading and in vitro release.

5 mg of $\text{Cu}_{2-x}\text{Se}@m\text{SiO}_2\text{-PEG}$ nanoparticles were dispersed in 10 mL of PBS solution (pH 7.4) containing DOX (0.15 mg/mL). The mixture was stirred at room temperature for 48 h under dark conditions. The DOX-loaded $\text{Cu}_{2-x}\text{Se}@m\text{SiO}_2\text{-PEG}$ ($\text{Cu}_{2-x}\text{Se}@m\text{SiO}_2\text{-PEG}/\text{DOX}$) nanocomposites were collected by centrifugation at 12000 rpm for 12 min and were washed several times with water until the supernatant became colorless. All supernatants were collected together. The amount of loaded DOX for $\text{Cu}_{2-x}\text{Se}@m\text{SiO}_2\text{-PEG}$ was analyzed by a UV-Vis spectrophotometer at 482 nm and calculated as bellow. Encapsulation efficiency = (weight of DOX loaded into the $\text{Cu}_{2-x}\text{Se}@m\text{SiO}_2\text{-PEG}$)/(initial weight of DOX), loading content = (weight of DOX loaded into the $\text{Cu}_{2-x}\text{Se}@m\text{SiO}_2\text{-PEG}$)/(weight of the $\text{Cu}_{2-x}\text{Se}@m\text{SiO}_2\text{-PEG}$ + DOX loaded into the $\text{Cu}_{2-x}\text{Se}@m\text{SiO}_2\text{-PEG}$). The release behaviors were performed at room temperature. Above-prepared $\text{Cu}_{2-x}\text{Se}@m\text{SiO}_2\text{-PEG}/\text{DOX}$ complexes were dispersed in 5 mL of buffer solution with ultrasonication at pH values of 7.4 and pH 4.8 respectively, and stirred at room temperature. At selected time intervals, the nanomaterials solutions were centrifuged (12,000 rpm, 10 min) and supernatants were withdrawn for analysis of DOX and the same volume of fresh buffers was added back to the residual nanomaterials. The amounts of the released DOX in the supernatant solutions were analyzed by a UV-Vis spectrometer at 482 nm. To study that the DOX could release increased from the nanoparticles under laser irradiation, release media solutions were irradiated with the NIR laser (980 nm, 0.72 W/cm²) for 5 min at predetermined time intervals, and then centrifuged and supernatants withdrawn for analysis of DOX.

2.8. Cell culture.

Cell culture was referenced method reported by the literatures.^{22,23,40} Human cervical carcinoma cell lines (HeLa) were continuously grown in 50 mL culture flask, incubated by DMEM medium supplemented with 10% heat-inactivated fetal bovine serum, 100 µg/mL streptomycin, 100 U/mL penicillin in a humidified incubator under 5% CO₂ at 37 °C.

2.9. In vitro cytotoxicity of the $\text{Cu}_{2-x}\text{Se}@m\text{SiO}_2\text{-PEG}$ nanoparticles.

The in vitro cytotoxicity was measured using the MTT assay in human cervical carcinoma cell line.^{22,28} HeLa cells were plated into a 96-well plate (1×10^4 cells per well) in a complete medium at 37 °C and 5% CO₂ for 24 h before the experiments. The culture medium was replaced and cells were incubated with complete medium containing the $\text{Cu}_{2-x}\text{Se}@m\text{SiO}_2\text{-PEG}$ core-shell nanoparticles at a series of concentrations at 37 °C with 5% CO₂ for further 24 h. Then the culture medium was replaced with fresh medium and MTT solution (10 µL, 5 mg/mL) was added to each well of the culture plate, and the cells were incubated in the CO₂ incubator for another 4 h. The cells then were lysed by the addition of 100 µL of DMSO. The spectrophotometric absorbance of formazan was measured using a plate reader at 570 nm. Four replicates were done for each treatment group.

2.10. In vitro chemo-photothermal therapy.

HeLa cells were plated into a 96-well plate (1×10^4 cells per well) in a complete medium at 37 °C and 5% CO₂ for 24 h before the experiments. The culture medium was replaced with complete medium containing the DOX, $\text{Cu}_{2-x}\text{Se}@m\text{SiO}_2\text{-PEG}/\text{DOX}$ and $\text{Cu}_{2-x}\text{Se}@m\text{SiO}_2\text{-PEG}$ at an equivalent DOX concentration. $\text{Cu}_{2-x}\text{Se}@m\text{SiO}_2\text{-PEG}$ and $\text{Cu}_{2-x}\text{Se}@m\text{SiO}_2\text{-PEG}/\text{DOX}$ have equivalent Cu⁺ concentration. After 4 h of incubation, the cells were washed by PBS to removed unbound material and replaced with fresh medium. The cells were treated with or without 980 nm laser (0.72 W/cm²) irradiation for 5 min, respectively, and then incubated at 37 °C with 5% CO₂ for further 20 h. MTT assay was also carried out to quantify the cell viabilities. Four replicates were done for each treatment group.

2.11. In vivo chemo-photothermal therapy.

The chemo-photothermal therapy test of cancer cells in vivo were respectively carried out by a modified method similar to reference.^{20,29} The osteosarcoma bearing mice were from Shanghai tenth people's hospital. When the tumors inside the mice had grown to 5-10 mm in diameter, the mice were randomly allocated into three groups. The mice were first anaesthetized by trichloroacetaldehyde hydrate (10 %) at a dosage of 40 mg/kg body weight. Then the mouse in group A was intratumorally injected with 0.10 mL of phosphate-buffered saline (PBS) solution containing $\text{Cu}_{2-x}\text{Se}@m\text{SiO}_2\text{-PEG}$ nanoparticles (400 µg/mL), the mouse in group B was intratumorally injected with 0.10 mL PBS solution containing $\text{Cu}_{2-x}\text{Se}@m\text{SiO}_2\text{-PEG}/\text{DOX}$ nanocomposites (400 µg/mL), while group C was intratumorally injected with 0.1 mL saline solution. After 1 h, the injected areas of mice from three groups were perpendicularly irradiated by the 980 nm wavelength laser devices at 0.72 W/cm² for 5 min. The temperature of the tumors surface was measured by a photothermal therapy-monitoring system GX-A300 (Shanghai Guixin Corporation). The mice were killed 8 h after photothermal therapy, and tumors were removed, embedded in paraffin, and cryo-sectioned into 4 µm slices. The slides were stained with hematoxylin/eosin (H&E). The slices were examined under a Zeiss Axiovert 40 CFL inverted fluorescence microscope, and images were captured with a Zeiss AxioCam MRc5 digital camera.

2.12 In vivo antitumor effect.

The osteosarcoma bearing mice

were from Shanghai Tenth People's Hospital. When the tumor volume inside the mice reached $\sim 85 \text{ mm}^3$. The mice were randomly allocated into four groups and intratumorally injected with 150 μL of PBS, DOX, $\text{Cu}_{2-x}\text{Se@mSiO}_2\text{-PEG}$, and $\text{Cu}_{2-x}\text{Se@mSiO}_2\text{-PEG/DOX}$ solutions (DOX 50 $\mu\text{g/mL}$, $\text{Cu}_{2-x}\text{Se@mSiO}_2\text{-PEG}$ 320 $\mu\text{g/mL}$). After injection, tumors were irradiated with the NIR light (980 nm, 0.72 W/cm^2) for 10 min. Tumor sizes were monitored per two days for 10 days. The length and width of the tumors were measured by a digital vernier caliper. The tumor volume was calculated according to the following formula: $\text{width}^2 \times \text{length}/2$.

3. RESULTS AND DISCUSSION

Fig 1 illustrates the synthetic process of the $\text{Cu}_{2-x}\text{Se@mSiO}_2\text{-PEG}$ core-shell nanoparticles and the theranostic principle based on the unique properties of $\text{Cu}_{2-x}\text{Se@mSiO}_2\text{-PEG}$ for cancer treatment. First, the Cu_{2-x}Se nanocrystals as photothermal agents were synthesized, and coated by mesoporous silica forming $\text{Cu}_{2-x}\text{Se@mSiO}_2$ core-shell nanoparticles. In order to enhance the biocompatibility and stability of $\text{Cu}_{2-x}\text{Se@mSiO}_2$ in aqueous solution, $\text{Cu}_{2-x}\text{Se@mSiO}_2$ nanoparticles were further modified by PEG-silane on their outermost surfaces, forming $\text{Cu}_{2-x}\text{Se@mSiO}_2\text{-PEG}$ core-shell nanoparticles. The anticancer drug DOX was loaded on mesoporous silica shell within the $\text{Cu}_{2-x}\text{Se@mSiO}_2\text{-PEG}$ core-shell nanoparticles, forming $\text{Cu}_{2-x}\text{Se@mSiO}_2\text{-PEG/DOX}$ nanocomposites. The $\text{Cu}_{2-x}\text{Se@mSiO}_2\text{-PEG/DOX}$ nanocomposites were internalized by cancer cells due to their good features. The Cu_{2-x}Se cores inside nanocomposites operate as NIR light absorbing agents, which can effectively convert NIR light into heat resulting in rapid release of DOX, thus dual therapeutic modes (photothermal therapy and chemotherapy) can be achieved by the NIR radiation and result in a synergistic effect for killing cancer cell.

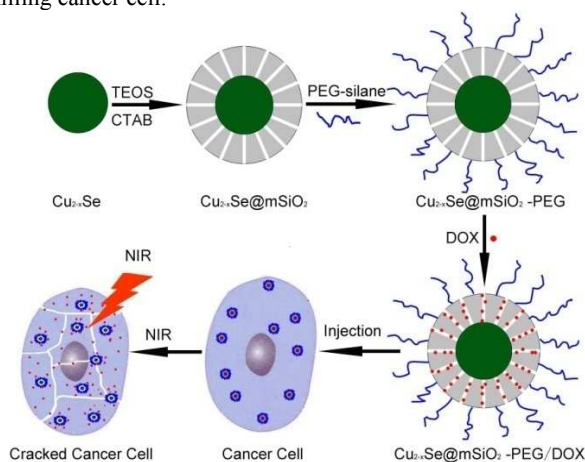


Fig. 1 Schematic illustration of $\text{Cu}_{2-x}\text{Se@mSiO}_2\text{-PEG}$ core-shell nanoparticles preparation and application as a difunctional treatment platform for cancer treatment.

The hydrophobic Cu_{2-x}Se nanoparticles were first synthesized according to a reported protocol³⁵ with some modifications. The transmission electron microscope (TEM) images of the obtained Cu_{2-x}Se nanocrystals showed an average diameter of $\sim 12 \text{ nm}$ and high crystallinity (Fig 2a, Fig S1a). Then, hydrophobic Cu_{2-x}Se nanoparticles were transferred into an aqueous phase by utilizing

cetyltrimethylammonium bromide (CTAB) to endow hydrophilic property and facilitate the SiO_2 coating. In the silica-coating process, CTAB formed a bilayer around the Cu_{2-x}Se nanocrystals and acted as an organic template for preparing $\text{Cu}_{2-x}\text{Se@mSiO}_2$ core-shell nanoparticles. The $\text{Cu}_{2-x}\text{Se@mSiO}_2\text{-PEG}$ core-shell nanoparticles (x is 0.42 measured by ICP) were obtained by modifying $\text{Cu}_{2-x}\text{Se@mSiO}_2$ nanoparticles with PEG-silane. Based on TEM images of the fabricated $\text{Cu}_{2-x}\text{Se@mSiO}_2\text{-PEG}$ core-shell nanoparticles (Figs 2b,c, Figs S1b,c), the Cu_{2-x}Se nanocrystals are completely encapsulated into mesoporous SiO_2 shell with an estimated thickness of $\sim 10 \text{ nm}$, and $\text{Cu}_{2-x}\text{Se@mSiO}_2\text{-PEG}$ nanoparticles have a diameter of $\sim 32 \text{ nm}$.

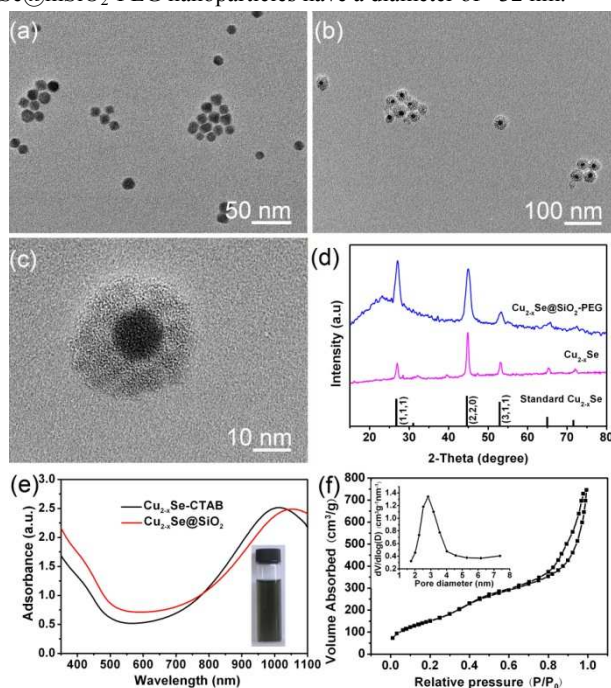


Fig. 2 TEM images of (a) Cu_{2-x}Se and (b,c) $\text{Cu}_{2-x}\text{Se@mSiO}_2\text{-PEG}$. (d) XRD patterns of the standard Cu_{2-x}Se (lower), as-synthesized Cu_{2-x}Se (middle) and $\text{Cu}_{2-x}\text{Se@mSiO}_2\text{-PEG}$ (upper). (e) Absorption spectra of $\text{Cu}_{2-x}\text{Se-CTAB}$ and $\text{Cu}_{2-x}\text{Se@mSiO}_2\text{-PEG}$, inset shows a photograph of $\text{Cu}_{2-x}\text{Se@mSiO}_2\text{-PEG}$ dispersion solution. (f) N_2 adsorption-desorption isotherms (inset: the pore diameter distribution) of $\text{Cu}_{2-x}\text{Se@mSiO}_2\text{-PEG}$ core-shell nanoparticles.

The phase structures of the as-obtained Cu_{2-x}Se nanocrystals and $\text{Cu}_{2-x}\text{Se@mSiO}_2\text{-PEG}$ nanoparticles were examined by XRD pattern, as shown in Fig 2d. Several well-defined characteristic peaks such as (1, 1, 1), (2, 2, 0) and (3, 1, 1) exhibit the cubic phase, referenced by standard Cu_{2-x}Se phase (JCPDS card no: 06-0680), while $\text{Cu}_{2-x}\text{Se@mSiO}_2\text{-PEG}$ nanoparticles have a wide and weak peak at about 23° which is clearly due to amorphous silica coating. The Cu_{2-x}Se and $\text{Cu}_{2-x}\text{Se@mSiO}_2\text{-PEG}$ nanoparticles were further investigated by high-resolution TEM (HRTEM). As shown in Fig S1a,d, interplane-distance of (111) crystal planes is 0.330 nm, corresponding to standard cubic Cu_{2-x}Se phase and other researches.⁴¹ It was proved that the Cu_{2-x}Se had cubic phase both before and after the silica coating. Since cubic phase is more stable for Cu_{2-x}Se ,⁴² it is advantageous to use Cu_{2-x}Se to acquire stable photothermal effect in photothermal therapy process. Absorption spectra of as-obtained Cu_{2-x}Se

CTAB and $\text{Cu}_{2-x}\text{Se}@m\text{SiO}_2\text{-PEG}$ are shown in Fig 2e. Both $\text{Cu}_{2-x}\text{Se-CTAB}$ and $\text{Cu}_{2-x}\text{Se}@m\text{SiO}_2\text{-PEG}$ nanoparticles show strong NIR region absorption. The as-prepared $\text{Cu}_{2-x}\text{Se-CTAB}$ nanoparticles have an absorbance peak at 1012 nm. After silica-shell coating, it exhibits a small red-shift (~ 24 nm). This phenomenon could be explained by the fact that the refractive index of the silica shell is larger than water.²⁸ The absorbance peak of $\text{Cu}_{2-x}\text{Se}@m\text{SiO}_2\text{-PEG}$ is close to the wavelength (980 nm) of excitation laser, which is advantageous for full usage of the SPR effect of materials, and enhancing photothermal efficiency.⁴³ Fig 2f showed the N_2 adsorption-desorption isotherm and pore size distribution (inset) of $\text{Cu}_{2-x}\text{Se}@m\text{SiO}_2\text{-PEG}$. The isotherm of $\text{Cu}_{2-x}\text{Se}@m\text{SiO}_2\text{-PEG}$ after CTAB extraction displays a typical type IV feature. The BET (Brunauer-Emmett-Teller) surface area and total pore volume of the core-shell nanoparticles were measured to be $579 \text{ m}^2/\text{g}$ and $1.15 \text{ m}^3/\text{g}$ respectively. The pore size distribution (Fig 2f, inset) exhibits a sharp peak centered at a mean value of 2.8 nm. Thus, $\text{Cu}_{2-x}\text{Se}@m\text{SiO}_2\text{-PEG}$ core-shell nanoparticles have large surface area and appropriate pore size, which are favorable for drug loading.

PEG modification of the silica shells can improve colloidal stability, decrease immunogenicity and enhance the tumor targeting efficiency for in vivo applications,^{28, 44} thus the $\text{Cu}_{2-x}\text{Se}@m\text{SiO}_2$ core-shell nanoparticles were further grafted with PEG-silane on their outmost surfaces via covalent bonding, forming the $\text{Cu}_{2-x}\text{Se}@m\text{SiO}_2\text{-PEG}$ core-shell nanoparticles. The Fourier transform infrared (FTIR) spectra of the $\text{Cu}_{2-x}\text{Se}@m\text{SiO}_2\text{-PEG}$ core-shell nanoparticles and PEG-silane reactant are shown in Fig S2. The adsorption bands at $2980\text{-}2845 \text{ cm}^{-1}$ and adsorption peaks at 1390 cm^{-1} are assigned to the stretching vibrations and deformation vibration of methylene (CH_2) respectively, in the long alkyl chain of the backbone of PEG.⁴⁵ Compared to PEG-silane reactant, the $\text{Cu}_{2-x}\text{Se}@m\text{SiO}_2\text{-PEG}$ nanoparticles have similar adsorption bands at same area, suggesting that the PEG is successfully grafted on the mesoporous silica surface. Besides, the $\text{Cu}_{2-x}\text{Se}@m\text{SiO}_2\text{-PEG}$ core-shell nanoparticles show excellent colloidal stability. After a period of 7 days, there is no aggregation and negligible absorption reduction in the NIR region during the storage of $\text{Cu}_{2-x}\text{Se}@m\text{SiO}_2\text{-PEG}$ core-shell nanoparticles in water (Fig S3).

As-prepared $\text{Cu}_{2-x}\text{Se}@m\text{SiO}_2\text{-PEG}$ nanoparticles show strong NIR absorption feature, making them a potential photothermal therapy agent. To investigate the photothermal effect generated by NIR laser irradiation, the temperatures of the solutions containing various concentrations of $\text{Cu}_{2-x}\text{Se}@m\text{SiO}_2\text{-PEG}$ were measured under irradiation of 980 nm laser with a safe power density ($0.72 \text{ W}/\text{cm}^2$). As shown in Fig 3a, the temperature of $\text{Cu}_{2-x}\text{Se}@m\text{SiO}_2\text{-PEG}$ aqueous solution at concentration of $200 \mu\text{g}/\text{mL}$ (48.9 ppm Cu^+) was raised from $25.0 \text{ }^\circ\text{C}$ to $45.3 \text{ }^\circ\text{C}$ after 480 s NIR irradiation. In comparison, the temperature of the control experiment of pure water ($0 \mu\text{g}/\text{mL}$) and Au nanorods (50 ppm Au) was only increased respectively by $4.3 \text{ }^\circ\text{C}$ and $14.2 \text{ }^\circ\text{C}$ after irradiated by the NIR laser under the same conditions (Fig S4), which indicating $\text{Cu}_{2-x}\text{Se}@m\text{SiO}_2\text{-PEG}$ nanoparticles have better photothermal effect than widely used Au nanorods when they are driven by 980 nm laser at same metal ion concentration. Moreover, the higher concentration of $\text{Cu}_{2-x}\text{Se}@m\text{SiO}_2\text{-PEG}$ nanoparticles, the higher the temperature elevation increased (Fig

3b). These data confirm that the $\text{Cu}_{2-x}\text{Se}@m\text{SiO}_2\text{-PEG}$ can effectively convert NIR light into fatal heat due to the strong SPR absorption of Cu_{2-x}Se core.²⁵

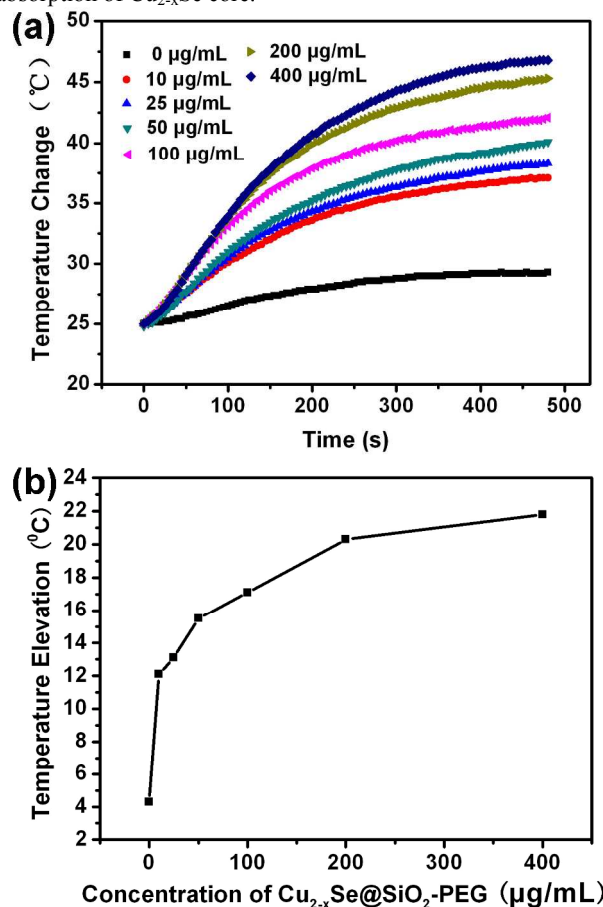


Fig.3 (a) Temperature change of the aqueous solution containing the $\text{Cu}_{2-x}\text{Se}@m\text{SiO}_2\text{-PEG}$ nanoparticles with different concentrations under irradiation of the 980 nm laser at a safe power density ($0.72 \text{ W}/\text{cm}^2$). (b) Plot of temperature elevation over a period of 480 s versus the aqueous dispersion of the $\text{Cu}_{2-x}\text{Se}@m\text{SiO}_2\text{-PEG}$ nanoparticles.

Based on the mesoporous shell structures, the $\text{Cu}_{2-x}\text{Se}@m\text{SiO}_2\text{-PEG}$ particles are expected to be suitable for anticancer drug delivery. DOX was loaded into the $\text{Cu}_{2-x}\text{Se}@m\text{SiO}_2\text{-PEG}$ nanoparticles by simply mixing DOX aqueous solutions for 48 h, and then repeated washing twice to remove unbound DOX, forming $\text{Cu}_{2-x}\text{Se}@m\text{SiO}_2\text{-PEG}/\text{DOX}$ nanocomposites, and the aqueous solution of which shows a bronzing color (Fig 4a, inset). After loaded with DOX, $\text{Cu}_{2-x}\text{Se}@m\text{SiO}_2\text{-PEG}/\text{DOX}$ complex still exhibits strong NIR absorbance of $\text{Cu}_{2-x}\text{Se}@m\text{SiO}_2\text{-PEG}$, and shows typical absorption peak of DOX near 480 nm region, which indicates the DOX has been successfully incorporated into the $\text{Cu}_{2-x}\text{Se}@m\text{SiO}_2\text{-PEG}$ core-shell nanoparticles (Fig 4a). The encapsulation efficiency and loading capacity of DOX on the $\text{Cu}_{2-x}\text{Se}@m\text{SiO}_2\text{-PEG}$ particles reached up to 61.27% and 15.53% (by weight) as determined by UV-vis, respectively. The loading content is higher than the present core-shell nanocomposites ($\text{Au}@m\text{SiO}_2$ core-shell nanostructures 14.5%,²⁷ $\text{Cu}_9\text{S}_5@m\text{SiO}_2\text{-PEG}$ core-shell nanocomposites 13.76%²⁹). The high encapsulation efficiency and loading capacity of DOX can

be assigned to large surface area and appropriate pore size of $\text{Cu}_{2-x}\text{Se@mSiO}_2\text{-PEG}$.

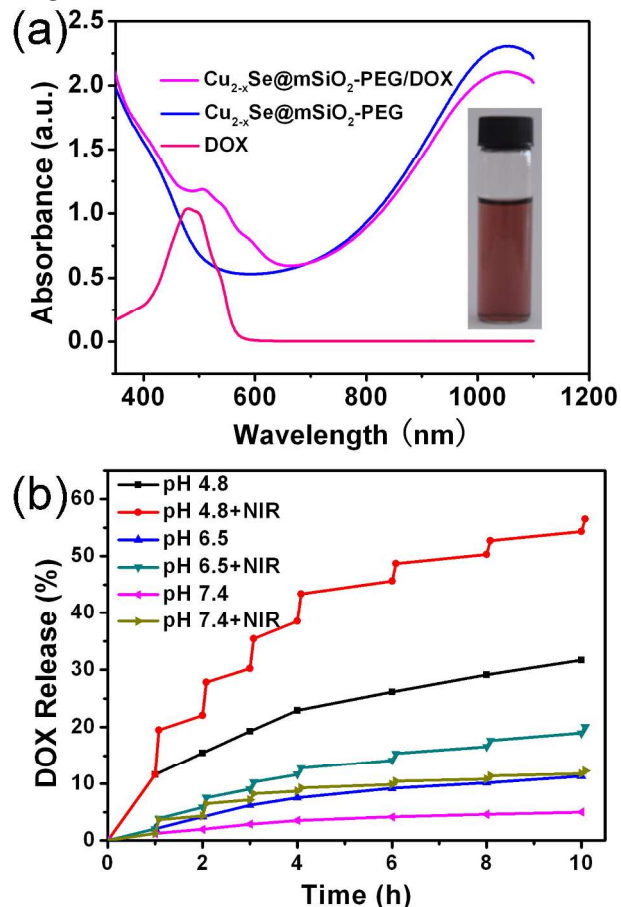
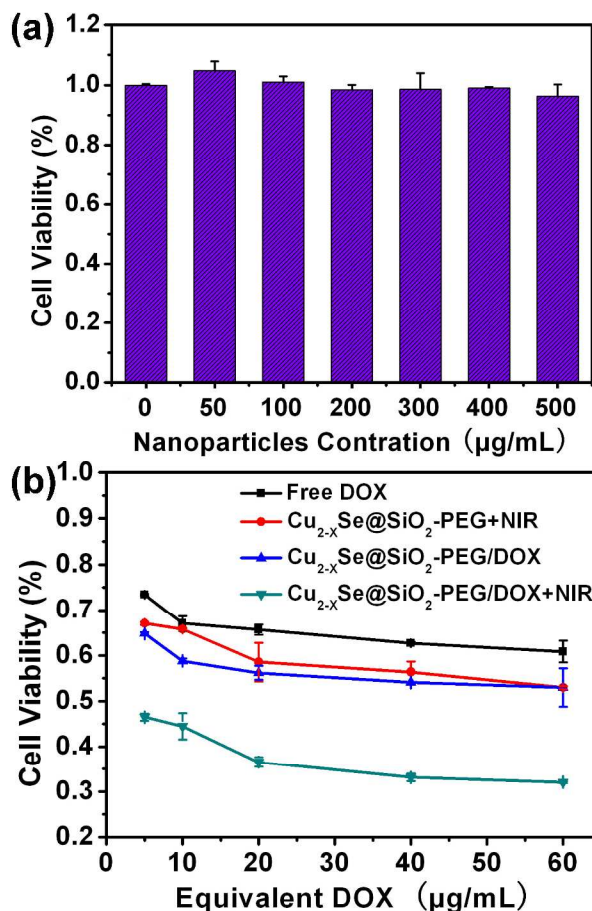


Fig. 4 (a) Absorption spectra of the DOX, $\text{Cu}_{2-x}\text{Se@mSiO}_2\text{-PEG}$ and $\text{Cu}_{2-x}\text{Se@mSiO}_2\text{-PEG/DOX}$ solutions. (b) The cumulative release kinetics from the $\text{Cu}_{2-x}\text{Se@mSiO}_2\text{-PEG/DOX}$ nanocomposites in phosphate-buffer saline (pH 7.4), phosphate-buffer saline (pH 6.5) and acetate buffer (pH 4.8) at room temperature with or without NIR laser irradiation by a safe power density (0.72 W/cm^2).

The DOX release from the $\text{Cu}_{2-x}\text{Se@mSiO}_2\text{-PEG}$ nanocomposites against buffer solution at pH 7.4, 6.5 and 4.8 was researched to simulate normal physiological environment, tumor cells environment and acidic cellular endosomes, respectively. As shown in Fig 4b, the release of DOX from the $\text{Cu}_{2-x}\text{Se@mSiO}_2\text{-PEG}$ nanoparticles strongly depended on the pH of the medium and the releasing time. Because DOX became more water soluble at low pH value due to the protonated daunosamine group,⁴⁶ much more rapid DOX release from $\text{Cu}_{2-x}\text{Se@mSiO}_2\text{-PEG}$ nanoparticles at low pH value. At pH 7.4, DOX molecules are barely released, indicating that $\text{Cu}_{2-x}\text{Se@mSiO}_2\text{-PEG}$ nanopatform releases very little DOX molecules in normal physiological environment and normal cells can be effectively avoided from hurt by DOX, but in tumor cells environment, DOX releases more rapidly and reaches 11.33% in 10h. At pH 4.8, DOX releases as high as 31.67%, which always occurs when the nanocomposites are endocytosed by tumor cells. Thus, such a pH-sensitive release of DOX from $\text{Cu}_{2-x}\text{Se@mSiO}_2\text{-PEG}$ is beneficial for cancer therapy.

Fig. 5 (a) Viabilities of HeLa cells incubated for 24 h with



nanoparticles. (b) Viabilities of HeLa cells after incubation with different concentrations of free DOX, $\text{Cu}_{2-x}\text{Se@mSiO}_2\text{-PEG}$ and $\text{Cu}_{2-x}\text{Se@mSiO}_2\text{-PEG/DOX}$ with or without 5 min of NIR irradiation (0.72 W/cm^2 , 980 nm). $\text{Cu}_{2-x}\text{Se@mSiO}_2\text{-PEG}$ and $\text{Cu}_{2-x}\text{Se@mSiO}_2\text{-PEG/DOX}$ have equivalent Cu^+ concentration at corresponding equal DOX point.

To investigate whether the NIR photothermal effect offered by Cu_{2-x}Se nanoparticles could trigger the DOX release, the release kinetics of DOX from the $\text{Cu}_{2-x}\text{Se@mSiO}_2\text{-PEG/DOX}$ under NIR laser irradiation was studied. During the DOX release process from the $\text{Cu}_{2-x}\text{Se@mSiO}_2\text{-PEG}$ nanoparticles in the buffer solution at pH = 4.8, 6.5 and 7.4, 5 min NIR laser irradiations (980nm , 0.72 W/cm^2) were given at 1.0, 2.0, 3.0, 4.0, 6.0, 8.0 and 10.0 h. As shown in Fig 4b, the first 5 min of NIR irradiation at 1.0 h increased the cumulative release of DOX from 11.6% to 19.5% at pH 4.8 and from 2.1% to 3.9% at pH 6.5. At other cycles, the same phenomena that a rapid release upon NIR irradiation and slow release rate without NIR irradiation was observed. At pH 4.8, the DOX cumulative release reached to 56.5% within 10 h after seven cycles of 5 min irradiation at given time intervals, while only 31.7% DOX was released without irradiation. At pH 6.5, an increase of 10 h DOX release from 10.3 to 20.1% was also achieved by NIR irradiation. The enhanced drug release under NIR irradiation can be attributed to heat generated by photothermal effect of $\text{Cu}_{2-x}\text{Se@mSiO}_2\text{-PEG}$ nanoparticles. The heat dissociates the strong interactions between DOX and SiO_2 ,²⁸ thus more DOX molecules are

released. These results demonstrate that the $\text{Cu}_{2-x}\text{Se}@m\text{SiO}_2\text{-PEG}$ have successfully achieved the drug controllable release by pH and NIR light.

As discussed above, $\text{Cu}_{2-x}\text{Se}@m\text{SiO}_2\text{-PEG}$ nanoparticles have excellent photothermal and drug delivery effects. But the ideal photothermal agent also should be nontoxic or low toxic for biological applications. So we first incubated HeLa cells with the $\text{Cu}_{2-x}\text{Se}@m\text{SiO}_2\text{-PEG}$ particles at different concentrations for 24 h and then tested the cell viabilities by using the 3-(4,5-dimethylthiazol-2-yl)-2,5-diphenyltetrazolium bromide (MTT) assay. No significant differences in the cell proliferation were observed in the absence or presence of $\text{Cu}_{2-x}\text{Se}@m\text{SiO}_2\text{-PEG}$ nanoparticles (Fig. 5a). Even at the highest tested dose of $\text{Cu}_{2-x}\text{Se}@m\text{SiO}_2\text{-PEG}$ nanoparticles (500 $\mu\text{g}/\text{mL}$), cell viability still remained approximately 96.3%. These data show that the aqueous dispersion of $\text{Cu}_{2-x}\text{Se}@m\text{SiO}_2\text{-PEG}$ nanoparticles (<500 $\mu\text{g}/\text{mL}$) can be considered to have low cytotoxicity.

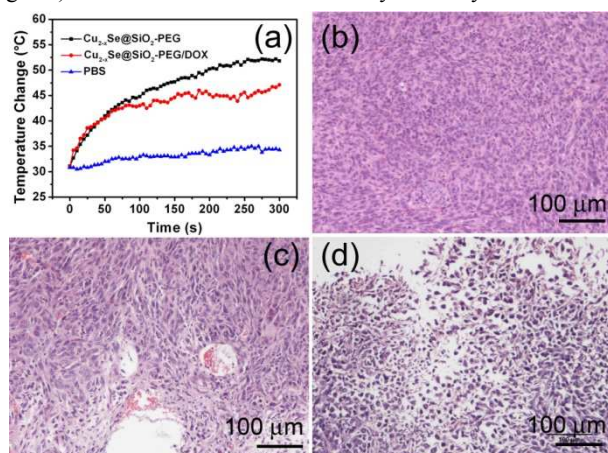


Fig. 6 (a) Plots of the temperature within the irradiated tumor area in three mice injected respectively with saline solution, $\text{Cu}_{2-x}\text{Se}@m\text{SiO}_2\text{-PEG}$ and $\text{Cu}_{2-x}\text{Se}@m\text{SiO}_2\text{-PEG/DOX}$ solution as a function of irradiation time, respectively, H&E-stained histological images of (b) injected saline solution, (c) injected $\text{Cu}_{2-x}\text{Se}@m\text{SiO}_2\text{-PEG}$ solution, and (d) injected $\text{Cu}_{2-x}\text{Se}@m\text{SiO}_2\text{-PEG/DOX}$ solution groups of mice after 5 minutes laser irradiation, respectively.

To investigate the effect of photothermal therapy, chemotherapy and their combination in vitro, HeLa cell incubated with different concentrations of free DOX, $\text{Cu}_{2-x}\text{Se}@m\text{SiO}_2\text{-PEG/DOX}$, $\text{Cu}_{2-x}\text{Se}@m\text{SiO}_2\text{-PEG}$ and $\text{Cu}_{2-x}\text{Se}@m\text{SiO}_2\text{-PEG/DOX}$ treated with or without NIR irradiation at safe power density (0.72 W/cm^2), and then the MTT assay was carried out to test the cell viability. The $\text{Cu}_{2-x}\text{Se}@m\text{SiO}_2\text{-PEG/DOX}$ nanoparticles demonstrated higher cytotoxicity than free DOX at the same concentrations (Fig. 5b). The $\text{Cu}_{2-x}\text{Se}@m\text{SiO}_2\text{-PEG/DOX}$ nanocomposites at an equivalent DOX concentration of 40 $\mu\text{g}/\text{mL}$ killed about 46% of cells, but free DOX killed only 37.3% cells at same condition. This result can be explained by that DOX-loaded nanoparticles can enter cancer cells more easily than free DOX.^{30,31} After uptake by cancer cells, the $\text{Cu}_{2-x}\text{Se}@m\text{SiO}_2\text{-PEG/DOX}$ nanocomposites experience a low-pH that induces rapid release of the loaded DOX inside the cells. After NIR laser irradiation (0.72 W/cm^2 , 980 nm), the $\text{Cu}_{2-x}\text{Se}@m\text{SiO}_2\text{-PEG/DOX}$ particles exhibited a higher cell-killing effect in HeLa cells at all tested concentrations than the

chemotherapy (without NIR irradiation) or the photothermal therapy (without DOX) alone. For example, 63.5% of the cells were killed by the $\text{Cu}_{2-x}\text{Se}@m\text{SiO}_2\text{-PEG/DOX}$ nanoparticles with NIR irradiation at an equivalent DOX concentration of 20 $\mu\text{g}/\text{mL}$. However, 43.9% of the cells were killed by the $\text{Cu}_{2-x}\text{Se}@m\text{SiO}_2\text{-PEG/DOX}$ nanoparticles without NIR irradiation. In the absence of DOX, the $\text{Cu}_{2-x}\text{Se}@m\text{SiO}_2\text{-PEG}$ (Cu^+ concentration is identical as $\text{Cu}_{2-x}\text{Se}@m\text{SiO}_2\text{-PEG/DOX}$) under NIR irradiation killed only 34.4% of the cells. Therefore, these results suggest that as-prepared $\text{Cu}_{2-x}\text{Se}@m\text{SiO}_2\text{-PEG}$ nanoparticles can act as a difunctional nanoplatform for chemo-photothermal therapy to effectively kill cancer driven by NIR irradiation at safe power density, and more importantly, the combination of photothermal therapy and chemotherapy demonstrates better therapeutic effects for cancer treatment than individual therapy.

The $\text{Cu}_{2-x}\text{Se}@m\text{SiO}_2\text{-PEG}$ core-shell nanoparticles have good photothermal conversion effect, high drug loading capacity, pH-dependent and NIR light-triggered drug release abilities, dual therapeutic modes (DOX release for chemotherapy and hyperthermia) in vitro characteristics. Because of the complexity of in vivo environment, the efficacy should be examined in vivo therapy before clinical trials in humans. The osteosarcoma bearing mice were from Shanghai tenth people's hospital. When the tumors inside the mice had grown to 5-10 mm in diameter, the mice were randomly allocated into three groups. The mouse in group A was intratumorally injected with 0.10 mL of the $\text{Cu}_{2-x}\text{Se}@m\text{SiO}_2\text{-PEG}$ nanoparticles' dispersion solution (400 $\mu\text{g}/\text{mL}$), the mouse in group B was intratumorally injected with 0.10 mL of the $\text{Cu}_{2-x}\text{Se}@m\text{SiO}_2\text{-PEG/DOX}$ (400 $\mu\text{g}/\text{mL}$) nanocomposites' dispersion solution, while group C was intratumorally injected with 0.1 mL saline solution. After 1 h, the injected areas of the mice from three groups were perpendicularly irradiated by the 980 nm wavelength laser devices (0.72 W/cm^2) for 5 min. For the mouse treated with saline solution, the surface temperature of the tumor increased only 3.5 $^{\circ}\text{C}$ during the entire irradiation process (Fig. 6a). In contrast, as to the $\text{Cu}_{2-x}\text{Se}@m\text{SiO}_2\text{-PEG}$ injected mouse, the tumor surface temperature increased rapidly from 31.1 $^{\circ}\text{C}$ to 48.1 $^{\circ}\text{C}$, and reached 51.8 $^{\circ}\text{C}$ after 300 s. The tumor surface temperature of $\text{Cu}_{2-x}\text{Se}@m\text{SiO}_2\text{-PEG/DOX}$ injected mouse increased to 47.1 $^{\circ}\text{C}$, a little lower than that of $\text{Cu}_{2-x}\text{Se}@m\text{SiO}_2\text{-PEG}$ injected mouse, but it was still high enough to kill the cancer cells in vivo. More importantly, the anticancer drug DOX could rapidly release from nanoparticles for chemotherapy because of the thermal effect. These results reveal that both $\text{Cu}_{2-x}\text{Se}@m\text{SiO}_2\text{-PEG}$ and $\text{Cu}_{2-x}\text{Se}@m\text{SiO}_2\text{-PEG/DOX}$ within the tumor can effectively adsorb and convert the NIR light to heat due to the deep penetration depth of 980 nm-wavelength laser light in biological tissues.^{20, 37,38}

The mice were killed 8 h after photothermal therapy, and tumors were removed, embedded in paraffin, and cryo-sectioned into 4 μm slices. The slides were stained with hematoxylin/eosin (H&E). The histopathological images of the mouse treated by saline (Fig. 6b, S5a) show almost no cell necrosis after irradiation. Because saline solution merely converted very little light to heat and temperature of tumor surface only increased 3.5 $^{\circ}\text{C}$, which is not high enough to kill the cancer cells. The histopathological images of the $\text{Cu}_{2-x}\text{Se}@m\text{SiO}_2\text{-PEG}$ treatment are shown in the Fig 6c and Fig S5b. Clearly, the common features of

thermonecrosis are presented on most areas of the examined tumor slide, such as cells shrinkage, loss of contact, coagulation, nuclear damage. Further, the histopathological images of the $\text{Cu}_{2-x}\text{Se@mSiO}_2\text{-PEG/DOX}$ treatment showed that almost all of the tumor tissue was necrotized, exhibiting degradation and corruption of the extracellular matrix of the tumor in the examined tumor slide (Fig 6d, Fig S5c). The enhanced cell necrosis proportion of the $\text{Cu}_{2-x}\text{Se@mSiO}_2\text{-PEG/DOX}$ treatment could probably be attributed to synergistic interaction between chemotherapy and photothermal therapy due to enhanced toxicity of DOX and hyperthermia,^{47,48} both of which were activated simultaneously by 980 nm laser.

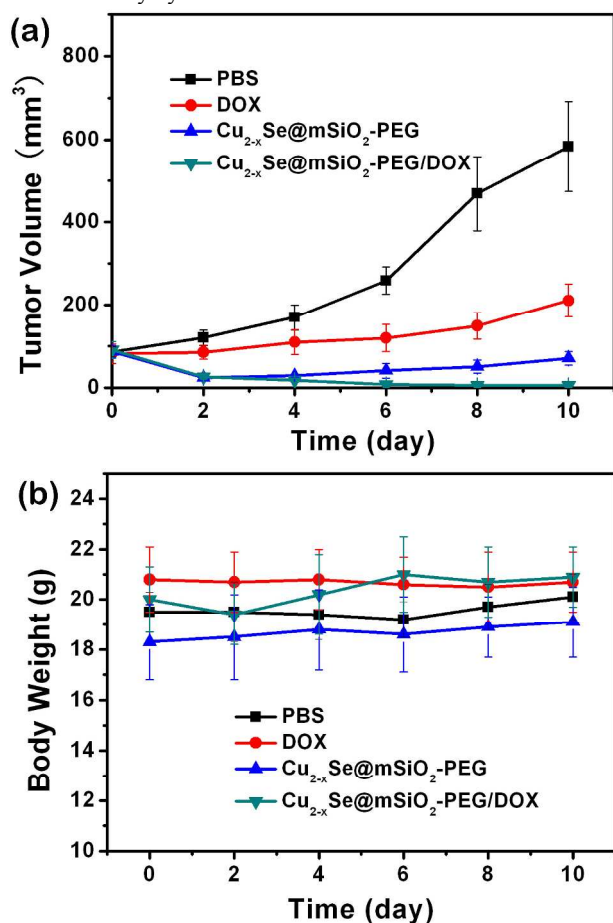


Fig. 7 (a) The osteosarcoma tumor growth curves of different groups after treatments. (b) Body weights of different groups mice after various treatments.

In order to further verify the enhanced anticancer effect of chemo-photothermal therapy by $\text{Cu}_{2-x}\text{Se@mSiO}_2\text{-PEG/DOX}$ nanocomposites in vivo, we then compared the in vivo therapeutic efficiency of saline, DOX, $\text{Cu}_{2-x}\text{Se@mSiO}_2\text{-PEG}$ and $\text{Cu}_{2-x}\text{Se@mSiO}_2\text{-PEG/DOX}$ by measuring tumor growth rates. The mice of osteosarcoma tumor model were randomly divided into four groups. The four groups were intratumorally injected into the tumor site, and then subjected to laser illumination (980 nm, 0.72 W/cm²) for 10 min. The tumor sizes and body weights of each group after treatments were then measured. The results demonstrated that the tumors treated with PBS grew obviously over time, suggesting that the osteosarcoma tumor growth was

not affected by laser irradiation (Fig.7a, S6). The growth of tumors was inhibited in a certain degree by free DOX as compared with PBS. The mean tumor size in the $\text{Cu}_{2-x}\text{Se@mSiO}_2\text{-PEG}$ group was much smaller than that of the PBS group, which demonstrates that the tumor growth could be obviously inhibited by just the photothermal effect of the $\text{Cu}_{2-x}\text{Se@mSiO}_2\text{-PEG}$ composites. The combination of the photothermal therapy and chemotherapy offered by $\text{Cu}_{2-x}\text{Se@mSiO}_2\text{-PEG/DOX}$ nanocomposites under laser irradiation showed significantly an enhanced antitumor activity and even resulted in complete eradication of tumor (Fig. S6). These results could probably be attributed to a synergistic effect between the chemotherapy and photothermal therapy due to enhanced cytotoxicity of DOX at elevated temperatures and higher heat sensitivity for the cells exposed to the DOX,^{47,48} and continuous release of the DOX from the $\text{Cu}_{2-x}\text{Se@mSiO}_2\text{-PEG/DOX}$ nanocomposites, inhibiting tumor growth for a long time. During the treatments, we also measured the body weight of the mice for all groups, because a high toxicity usually leads to weight loss. For all groups, no obvious weight loss was found (Fig.7b), implying that the toxicity of treatments was low. Therefore, the as-prepared $\text{Cu}_{2-x}\text{Se@mSiO}_2\text{-PEG}$ nanoparticles driven by the NIR irradiation at the safe power density not only have good photothermal treatment ability, but also act as drug delivery carriers for cancer chemotherapy. Importantly, the combination of the photothermal therapy and chemotherapy significantly improves the therapeutic efficacy, and demonstrates better therapeutic effects for cancer treatment than individual therapy in vivo. To the best of our knowledge, this is the first time to fabricate a combination of photothermal therapy and chemotherapy based on the Cu_{2-x}Se nanomaterials. These results revealed that the DOX loaded $\text{Cu}_{2-x}\text{Se@mSiO}_2\text{-PEG}$ core-shell nanoparticles driven by NIR irradiation at the safe power density were a powerful agent for combining chemotherapy and photothermal therapy of cancer in vivo.

4. Conclusions

In summary, the hydrophilic $\text{Cu}_{2-x}\text{Se@mSiO}_2\text{-PEG}$ core-shell nanoparticles were successfully prepared, which possess high photothermal conversion effect and excellent biocompatibility in vitro. Moreover, the outer biocompatible mesoporous SiO_2 shell can protect the photothermal utilization of Cu_{2-x}Se core in complex biological environments and serve as a drug carrier for loading DOX for chemotherapy of cancer.

The release of DOX from the $\text{Cu}_{2-x}\text{Se@mSiO}_2\text{-PEG}$ core-shell nanoparticles can be triggered by pH and NIR light, resulting in a synergistic effect for killing cancer cell. Importantly, we have demonstrated that $\text{Cu}_{2-x}\text{Se@mSiO}_2\text{-PEG/DOX}$ nanocomposites driven by the NIR radiation with safe power density showed significant enhancement of therapy effects on cancer cells than individual therapy approaches in vitro and in vivo. Therefore, $\text{Cu}_{2-x}\text{Se@mSiO}_2\text{-PEG/DOX}$ core-shell nanocomposites integrate the photothermal therapy and chemotherapy and have a great potential use for cancer therapy.

Acknowledgements

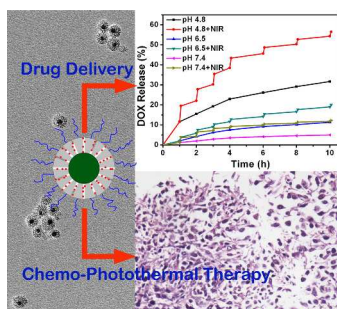
This work was financially supported by the National Natural Science Foundation of China (Grant Nos. 21171035 and 51302035), the Key Grant Project of Chinese Ministry of Education (Grant No. 313015), the PhD Programs Foundation of the Ministry of Education of China (Grant Nos. 20110075110008 and 20130075120001), the National 863 Program of China (Grant No. 2013AA031903), the Science and Technology Commission of Shanghai Municipality (Grant No. 13ZR1451200), the Fundamental Research Funds for the Central Universities, Program for Changjiang Scholars and Innovative Research Team in University (Grant No. IRT1221), the Shanghai Leading Academic Discipline Project (Grant No. B603), and the Program of Introducing Talents of Discipline to Universities (No. 111-2-04).

Notes and references

- ¹⁵ ^a State Key Laboratory for Modification of Chemical Fibers and Polymer Materials, College of Materials Science and Engineering, Donghua University, Shanghai, China. E-mail: hu.junqing@dhu.edu.cn
- ^b College of Chemistry and Chemical Engineering, Shanghai University of Engineering Science, Shanghai, China.
- ²⁰ ^c Department of Orthopaedics, Shanghai First People's Hospital, Shanghai Jiaotong University, 100 Haining Road, Hongkou District, Shanghai, China.
- ^d Center of Super-Diamond and Advanced Films (COSDAF), Department of Physics and Materials Science, City University of Hong Kong, Hong Kong
- ^e College of Chemistry, Chemical Engineering and Biotechnology, Donghua University, Shanghai, China.
- † Electronic Supplementary Information (ESI) available: See DOI: 10.1039/b000000x/
- ‡ These authors contributed equally.
1. K. Yang, H. Xu, L. Cheng, C. Sun, J. Wang and Z. Liu, *Adv. Mater.*, 2012, **24**, 5586-5592.
 2. Z. Zha, X. Yue, Q. Ren and Z. Dai, *Adv. Mater.*, 2013, **25**, 777-782.
 3. Y. Hu, L. Meng, L. Niu and Q. Lu, *ACS Appl. Mater. Interfaces*, 2013, **5**, 4586-4591.
 4. P. Matteini, F. Tatini, L. Luconi, F. Ratto, F. Rossi, G. Giambastiani and R. Pini, *Angew. Chem. Int. Ed.*, 2013, **52**, 5956-5960.
 5. J. L. Li, D. Day and M. Gu, *Adv. Mater.*, 2008, **20**, 3866-3871.
 6. C. Ungureanu, R. Kroes, W. Petersen, T. A. M. Groothuis, F. Ungureanu, H. Janssen, F. W. B. van Leeuwen, R. P. H. Kooyman, S. Manohar and T. G. van Leeuwen, *Nano Lett.*, 2011, **11**, 1887-1894.
 7. W. Dong, Y. Li, D. Niu, Z. Ma, J. Gu, Y. Chen, W. Zhao, X. Liu, C. Liu and J. Shi, *Adv. Mater.*, 2011, **23**, 5392-5397.
 8. J. Kim, S. Park, J. E. Lee, S. M. Jin, J. H. Lee, I. S. Lee, I. Yang, J.S. Kim, S. K. Kim, M.-H. Cho and T. Hyeon, *Angew. Chem. Int. Ed.*, 2006, **45**, 7754-7758.
 9. L. Au, D. Zheng, F. Zhou, Z.-Y. Li, X. Li and Y. Xia, *Acs Nano*, 2008, **2**, 1645-1652.
 10. S. E. Skrabalak, J. Chen, L. Au, X. Lu, X. Li and Y. Xia, *Adv. Mater.*, 2007, **19**, 3177-3184.
 11. M. S. Yavuz, Y. Cheng, J. Chen, C. M. Cobley, Q. Zhang, M. Rycenga, J. Xie, C. Kim, K. H. Song, A. G. Schwartz, L. V. Wang and Y. Xia, *Nat. Mater.*, 2009, **8**, 935-939.
 12. J. Chen, C. Glaus, R. Laforest, Q. Zhang, M. Yang, M. Gidding, M. J. Welch and Y. Xia, *Small*, 2010, **6**, 811-817.
 13. H. Xiaoqing, T. Shaoheng, M. Xiaoliang, D. Yan, C. Guangxu, Z. Zhiyou, R. Fangxiong, Y. Zhilin and Z. Nanfeng, *Nat. Nanotechnol.*, 2011, **6**, 28-32.
 14. S. Tang, X. Huang and N. Zheng, *Chem. Commun.*, 2011, **47**, 3948-3950.
 15. H. K. Moon, S. H. Lee and H. C. Choi, *Acs Nano*, 2009, **3**, 3707-3713.

16. J. T. Robinson, K. Welsher, S. M. Tabakman, S. P. Sherlock, H. Wang, R. Luong and H. Dai, *Nano Res.*, 2010, **3**, 779-793.
17. K. Yang, L. Hu, X. Ma, S. Ye, L. Cheng, X. Shi, C. Li, Y. Li and Z. Liu, *Adv. Mater.*, 2012, **24**, 1868-1872.
18. K. Yang, S. Zhang, G. Zhang, X. Sun, S.-T. Lee and Z. Liu, *Nano Letters*, 2010, **10**, 3318-3323.
19. Y. Ma, S. Tong, G. Bao, C. Gao and Z. Dai, *Biomaterials*, 2013, **34**, 7706-7714.
20. Z. Chen, Q. Wang, H. Wang, L. Zhang, G. Song, L. Song, J. Hu, H. Wang, J. Liu, M. Zhu and D. Zhao, *Adv. Mater.*, 2013, **25**, 2095-2100.
21. M. Zhou, R. Zhang, M. Huang, W. Lu, S. Song, M. P. Melancon, M. Tian, D. Liang and C. Li, *J. Am. Chem. Soc.*, 2010, **132**, 15351-15358.
22. Q. Tian, M. Tang, Y. Sun, R. Zou, Z. Chen, M. Zhu, S. Yang, J. Wang, J. Wang and J. Hu, *Adv. Mater.*, 2011, **23**, 3542-3547.
23. Q. Tian, F. Jiang, R. Zou, Q. Liu, Z. Chen, M. Zhu, S. Yang, J. Wang, J. Wang and J. Hu, *Acs Nano*, 2011, **5**, 9761-9771.
24. Q. Tian, J. Hu, Y. Zhu, R. Zou, Z. Chen, S. Yang, R. Li, Q. Su, Y. Han and X. Liu, *J. Am. Chem. Soc.*, 2013, **135**, 8571-8577.
25. C. M. Hessel, V. P. Pattani, M. Rasch, M. G. Panthani, B. Koo, J. W. Tunnell and B. A. Korgel, *Nano Lett.*, 2011, **11**, 2560-2566.
26. K. Yang, J. Wan, S. Zhang, B. Tian, Y. Zhang and Z. Liu, *Biomaterials*, 2012, **33**, 2206-2214.
27. Z. Zhang, L. Wang, J. Wang, X. Jiang, X. Li, Z. Hu, Y. Ji, X. Wu and C. Chen, *Adv. Mater.*, 2012, **24**, 1418-1423.
28. S. Shen, H. Tang, X. Zhang, J. Ren, Z. Pang, D. Wang, H. Gao, Y. Qian, X. Jiang and W. Yang, *Biomaterials*, 2013, **34**, 3150-3158.
29. G. Song, Q. Wang, Y. Wang, G. Lv, C. Li, R. Zou, Z. Chen, Z. Qin, K. Hou, R. Hu and J. Hu, *Adv. Funct. Mater.*, 2013, **23**, 4281-4292.
30. W. Fang, S. Tang, P. Liu, X. Fang, J. Gong and N. Zheng, *Small*, 2012, **8**, 3816-3822.
31. W. Fang, J. Yang, J. Gong and N. Zheng, *Adv. Funct. Mater.*, 2012, **22**, 842-848.
32. Y. Wang, K. Wang, J. Zhao, X. Liu, J. Bu, X. Yan and R. Huang, *J. Am. Chem. Soc.*, 2013, **135**, 4799-4804.
33. M. Zheng, C. Yue, Y. Ma, P. Gong, P. Zhao, C. Zheng, Z. Sheng, P. Zhang, Z. Wang and L. Cai, *Acs Nano*, 2013, **7**, 2056-2067.
34. C. Wang, H. Xu, C. Liang, Y. Liu, Z. Li, G. Yang, H. Cheng, Y. Li and Z. Liu, *Acs Nano*, 2013, **7**, 6782-6795.
35. X. Liu, X. Wang, B. Zhou, W. C. Law, A. N. Cartwright and M. T. Swihart, *Adv. Funct. Mater.*, 2013, **23**, 1256-1264.
36. Z. L. Jiang, B. Dong, B. T. Chen, J. Wang, L. Xu, S. Zhang and H. W. Song, *Small*, 2013, **9**, 604-612.
37. Z. Chen, L. Zhang, Y. Sun, J. Hu and D. Wang, *Adv. Funct. Mater.*, 2009, **19**, 3815-3820.
38. L. Zhang, Q. Tian, W. Xu, X. Kuang, J. Hu, M. Zhu, J. Liu and Z. Chen, *J. Mater. Chem.*, 2012, **22**, 18156-18163.
39. Y.K. Peng, C.W. Lai, C.L. Liu, H.C. Chen, Y.H. Hsiao, W.L. Liu, K.C. Tang, Y. Chi, J.K. Hsiao, K.E. Lim, H.E. Liao, J.J. Shyue and P.T. Chou, *Acs Nano*, 2011, **5**, 4177-4187.
40. Q. Chen, K. Li, S. Wen, H. Liu, C. Peng, H. Cai, M. Shen, G. Zhang and X. Shi, *Biomaterials*, 2013, **34**, 5200-5209.
41. J. Choi, N. Kang, H. Y. Yang, H. J. Kim and S. U. Son, *Chem. Mater.*, 2010, **22**, 3586-3588.
42. J.J. Wang, D.J. Xue, Y.G. Guo, J.S. Hu and L.J. Wan, *J. Am. Chem. Soc.*, 2011, **133**, 18558-18561.
43. H. Chen, L. Shao, T. Ming, Z. Sun, C. Zhao, B. Yang and J. Wang, *Small*, 2010, **6**, 2272-2280.
44. A. S. Karakoti, S. Das, S. Thevuthasan and S. Seal, *Angew. Chem. Int. Ed.*, 2011, **50**, 1980-1994.
45. V. Cauda, C. Argyo and T. Bein, *J. Mater. Chem.*, 2010, **20**, 8693-8699.
46. X. C. Qin, Z. Y. Guo, Z. M. Liu, W. Zhang, M. M. Wan and B. W. Yang, *J. Photochem. Photobiol., B*, 2013, **120**, 156-162.
47. S. M. Lee, H. Park and K. H. Yoo, *Adv. Mater.*, 2010, **22**, 4049-4053.
48. H. Park, J. Yang, J. Lee, S. Haam, I. H. Choi and K. H. Yoo, *Acs Nano*, 2009, **3**, 2919-2926.

TOC



A difunctional nanoplatform based on the Cu_{2-x}Se@mSiO₂-5 PEG core-shell nanoparticles demonstrates an excellent biocompatibility and can be used for combining photothermal- and chemotherapies driven by the NIR light radiation with a safe power density.